Dynamic interaction of multiple delaminations and core damage in composite sandwich beams

Andrea Cavicchi, Roberta Massabò

Department of Civil, Environmental and Architectural Engineering,
University of Genova, Italy
E-mail: *cavicchi@dicat.unige.it, roberta.massabo@unige.it*

Keywords: Composite sandwich beams, damage mechanisms, dynamic loading.

SUMMARY. The paper deals with the nonlinear response of composite sandwich beams subject to static and dynamic out-of-plane loading. The internal structure of composite sandwich systems gives rise to complex damage and failure mechanisms. The objective of the study is to analyse two specific damage mechanisms, namely skin delamination and core crushing, and to investigate how they interact and what are the effects of such interactions on the mechanical behaviour of the system. The study refers to the model system of a sandwich beam that is continuously supported by a rigid plane and subject to a time dependent out-of-plane loading. The problem is studied using the schematic of a multiply delaminated beam on a nonlinear Winkler foundation.

1 INTRODUCTION

The combination of high strength, high stiffness and light weight makes composite sandwiches an attractive material system for naval, aerospace, transportation and other structural applications. Many of these applications are characterized by the presence of severe dynamic loads (for example due to explosions, gust and sonic boom pulses or high velocity impact) and require high damage resistance and tolerance and high energy absorption capabilities. Understanding the behaviour of sandwich systems under such type of loads and defining the conditions that minimize their negative effects while optimizing strength, energy dissipation and other mechanical properties is an important goal.

Experimental results [1-4] show that the internal structure of sandwich systems gives rise to complex damage and failure mechanisms due to the interaction of basic mechanisms such as skin and core-skin delamination, local indentation with core crushing, shear failure of the core, skin wrinkling and compressive failure of the skin. While several studies have been conducted to analyse the different failure modes and define failure maps in order to optimize the sandwich design [e.g. 5,6], the problem of the interaction of the different damage mechanisms and its effects on damage propagation and mechanical performance under dynamic loading conditions is not yet fully understood.

Multiple delamination is a dominant failure mechanism of laminated sheets when they are subject to dynamic out-of-plane loadings. It was shown in [7-8] that static and dynamic interactions between delamination cracks control their propagation and have important effects on the overall mechanical response and damage resistance. Different combinations of shielding and amplification phenomena (i.e., increase/decrease of fracture parameters with respect to the values for the cracks alone in the system) deeply affect the propagation of damage.

In sandwich beams, delaminations may arise between the laminae of the skin and also at the core-skin interface. Their static and dynamic interaction is expected to be deeply affected by the presence of the core whose non-linear elastic-plastic behaviour also plays a fundamental role in controlling how the energy from a dynamic load is distributed and dissipated in the structure.

The objective of this study is to analyse how the skin-core interaction affects the interaction and propagation of multiple delaminations in the skin and the evolution of plastic deformations in the core. The analyses refer to the model system of a sandwich beam that is continuously supported by a rigid plane and subject to time dependent out-of-plane loading. In this configuration overall bending and shear are not present and the analyses can focus on the local damage phenomena. The delaminated upper face sheet, which is subjected to the external load, is decomposed into Timoshenko sub-beams while the core is modelled as a non-linear Winkler foundation. Static and dynamic analyses are performed and the effects of the initial position and size of the delaminations and of the constitutive parameters of skin and core on damage propagation are analysed.

2 THEORETICAL MODELS

A sandwich beam with a rectangular cross section, composite face sheets, a homogeneous core and subject to out-of-plane loading is studied (Fig. 1a). The beam is assumed to be continuously supported by a rigid plane so that overall bending and shear are absent. The upper face of the sandwich is modelled as a multiply delaminated beam resting on a nonlinear elastic-plastic Winkler foundation that describes the compressive yielding response of the core (Fig.1b-c).

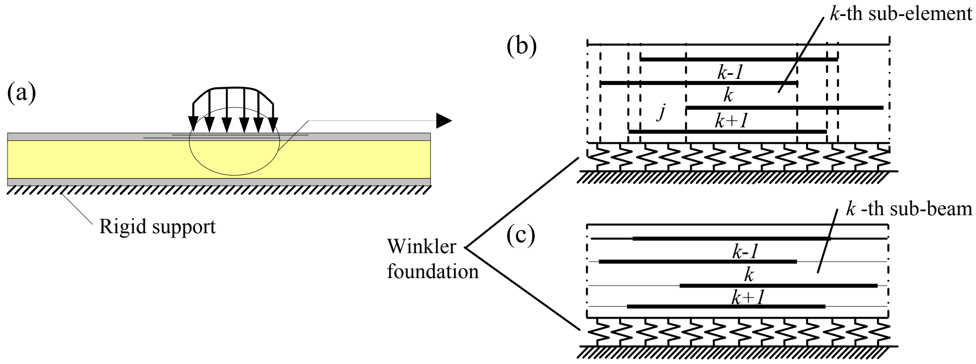

Fig.1 (a) Schematic of the problem and sub-beam subdivision of the face sheet in (b) the static and (c) the dynamic models.

The delaminated beam is subdivided into sub-beams using two different subdivision schemes for the static and the dynamic problems. In the static model the subdivision is defined by vertical sections at the crack tip positions and longitudinal sections along the delamination planes (Fig. 1b). In the dynamic model the subdivision is defined by longitudinal sections at the delamination planes (Fig. 1c). In both models the sub-beams are described by first order shear deformation beam theory. The generic sub-beam k (sub-beams are numbered from top to bottom and from left to right) has height h_k and its cross sectional moment of inertia and area per unit width are $I_k = h_k^3/12$ and $S_k = h_k$. The beam mass density is ρ_m. The generalized displacements of its centroidal axis are the axial and transverse displacements u_k and w_k and the rotation φ_k. The stress resultants per unit width are the axial force N_k, shear force V_k and bending moment M_k. The compatibility equations are:

$$\varphi_k = -w_k' + \gamma_k , \quad \varepsilon_k = u_k', \quad \chi_k = \varphi_k', \tag{1}$$

where ε_k, γ_k, and κ_k are the axial and shear deformations and the bending curvature and the superscript $'$ indicates a spatial derivative with respect to the longitudinal coordinate. The constitutive relationships are:

$$N_k = A_k \varepsilon_k\ ,\ M_k = D_k \chi_k\ ,\ V_k = G_k \gamma_k\ , \tag{2}$$

where D_k, A_k and G_k are the bending, extensional and shear stiffnesses of the sub-beam defined using lamination theory from the elastic constants and geometry of the laminae comprising the sub-beam. Each sub-beam is assumed to be globally orthotropic with principal material axes parallel to the longitudinal and transversal principal axes of the beam. In all the applications that follow, the beam is homogeneous and isotropic with Young modulus E and thickness h.

Normal and tangential tractions T^N and T^S act along the lower (subscript $k,k+1$) and upper (subscript k-1,k) surfaces of the k-th sub-beam. They may represent externally applied tractions on the beam surfaces, contact and cohesive tractions between the sub-beams or the action of the core. Equilibrium of sub-beam k is given by:

$$M_k' - V_k - 1/2\, h_k \left(T_{k,k+1}^S + T_{k-1,k}^S \right) = \rho_m I_k \ddot{\varphi}_k\ , \tag{3}$$

$$V_k' - T_{k,k+1}^N + T_{k-1,k}^N = \rho_m S_k \ddot{w}_k\ , \tag{4}$$

$$N_k' - T_{k,k+1}^S + T_{k-1,k}^S = \rho_m S_k \ddot{u}_k\ , \tag{5}$$

where the terms on the right hand sides account for the inertia of the sub-beam and the dot indicates a derivative with respect to time. In the static model the right hand sides are equal to zero.

The interaction between the generic sub-beams k and $k+1$ is described by interface laws $T_{k,k+1}^N\left(w_{k,k+1}^N, w_{k,k+1}^S\right)$ and $T_{k,k+1}^S\left(w_{k,k+1}^N, w_{k,k+1}^S\right)$ that relate the interfacial tractions, $T_{k,k+1}^N$ and $T_{k,k+1}^S$ to the interfacial opening and sliding displacements

$$w_{k,k+1}^N = w_{k+1} - w_k\ , \quad w_{k,k+1}^S = \left[u_{k+1} + \varphi_{k+1} h_{k+1}/2\right] - \left[u_k - \varphi_k h_k/2\right] \tag{6}$$

and depend on the specific behavior that the interface is called to describe in the model. The interface laws are approximated by piecewise linear curves.

When the interface law is used to represent perfect adhesion between sub-beams in the intact portions of the skin in the dynamic model, it is defined by a linear elastic branch up to a critical value. The normal and tangential stiffnesses are chosen to be very high to minimize errors due to the introduction of fictitious compliant surfaces in the body. The law also directly controls crack evolution when the material is assumed to be perfectly brittle.

Both static and dynamic models assume elastic normal contact between the sub-beams along the delamination surfaces and neglect friction. The interfacial tractions are given by $T_{k,k+1}^N = -K_{k,k+1}^c w_{k,k+1}^N$ and $T_{k,k+1}^S = 0$, where

$$K_{k,k+1}^c = \mathrm{H}\left(-w_{\mathrm{k,k+1}}^N\right) \frac{2E_T}{h_k + h_{k+1}}\ , \tag{7}$$

E_T is the through-thickness modulus of the sub-beams and $\mathrm{H}(.)$ is the Heaviside step function ($\mathrm{H}(\varsigma) = \{\ 1 \text{ if } \varsigma > 0,\ 0 \text{ otherwise}\ \}$).

The interaction between the lowest sub-beams and the Winkler foundation is described by an interface law that relates the relative displacements w_f^N and $w_f^S = u_f + \varphi_f h_f/2$ at the core-skin interface (f is a generic sub-beam lying on the foundation) to the normal T_f^N and shear T_f^S

tractions of the foundation. In the applications presented here $T_f^S = 0$. The cohesive law $T_f^N = T_f^N\left(w_f^N\right)$ is defined as piecewise linear function of the interface normal displacement. When core crushing is described by an elastic-plastic law, linear elastic unloading is assumed. Elastic-perfectly plastic behaviour of the core is assumed in the applications discussed in section 6.

3 DELAMINATION PROPAGATION

The delaminations are assumed to propagate collinearly in the matrix rich regions between the plies. In the static model the energy release rate of each delamination is calculated using the J-integral. The expression for a crack tip that separates beam segments *j* (ahead of the tip), *k* and *k*+1 (in the wake of the crack, Fig. 1b) is [9]:

$$\mathcal{G} = \mathrm{J} = \frac{1}{2}\left(\sum_{i=k}^{k+1}\left(\frac{M_i^2}{EI_i} + \frac{6}{5}\frac{V_i^2}{Gh_i} + \frac{N_i^2}{Eh_i} - 2V_i\Delta\varphi_i\right) - \frac{M_j^2}{EI_j} - \frac{6}{5}\frac{V_j^2}{Gh_j} - \frac{N_j^2}{Eh_j}\right) \tag{8}$$

where the stress resultants are calculated at the sub-beam sections at the crack tip and $\Delta\varphi_i$ are beam segments root rotations, namely the relative elastic rotations between the crack tip sections of the sub-beams *k* and *k*+1 and the sub-beam *j* [9].

In the dynamic model, delamination propagation is controlled by the interface law defined along the interface in the intact part of the beam. Critical mode I, w_0^N, and mode II, w_0^S, interfacial displacements define the end of the initial elastic steep branch used in the intact part of the beam. Softening branches following the initial linear elastic branch can then be used to describe cohesive fracture of the interface.

In this paper perfectly brittle fracture is assumed. The interfacial tractions are then assumed to vanish beyond the critical interfacial displacements and the areas under the cohesive traction-displacement laws represent the mode I and mode II fracture energies of the interface $\mathcal{G}_{Icr} = 1/2\, k_{k,k+1}^N (w_0^N)^2$ and $\mathcal{G}_{IIcr} = 1/2\, k_{k,k+1}^S (w_0^S)^2$. w_0^N and w_0^S are small enough to satisfy small scale yielding conditions [10-13]. Failure envelopes for mixed-mode fracture are then defined in terms of relative crack displacements or energy release rate components:

$$\left(H(w_{k,k+1}^N)\frac{w_{k,k+1}^N}{w_0^N}\right)^r + \left|\frac{w_{k,k+1}^S}{w_0^S}\right|^r = 1 \quad \text{or} \quad \left(\frac{\mathcal{G}_I}{\mathcal{G}_{Icr}}\right)^{r-1} + \left(\frac{\mathcal{G}_{II}}{\mathcal{G}_{IIcr}}\right)^{r-1} = 1, \tag{9}$$

where $r = 2$ is assumed in the examples of section 6.

4 SOLUTION OF THE STATIC MODEL

The solution of the static model is obtained by considering sub-sets of stacked sub-beams each one characterized by a uniform state of contact or cohesion at each interface along the longitudinal axis. For each sub-set a semi-analythical is obtained that describes static and kinematic fields of each sub-set as a function of its boundary conditions; closed form solutions are available with a maximum of two delaminations. The imposition of continuity conditions between horizontally adjacent sub-sets and of the overall boundary conditions of the delaminated beam leads to the rigorous reformulation of the initial differential equilibrium problem as a discrete problem to be solved numerically. An initial contact/cohesion state is assumed to start an iterative procedure where the contact/cohesion state is checked and updated at each iteration until convergence is obtained. If the loading conditions or the progression of damage induce unloading of the nonlinear foundation in its plastic phase, the problem requires an incremental approach.

5 SOLUTION OF THE DYNAMIC MODEL

In the dynamic model, the solution is found by discretizing the problem using unidimensional space and time grids and applying a finite difference numerical scheme with second order accuracy. The governing equations for all beam sections corresponding to each grid point are combined into a single matrix equation and boundary conditions are applied with all derivatives approximated as one-sided differences. The final matrix equation at time step *n* is of the form

$$\mathbf{M}\ddot{\mathbf{v}}^{(n)} = \mathbf{K}^{(n)}\mathbf{v}^{(n)} + \mathbf{F}^{(n)} \tag{10}$$

where $\mathbf{v}^{(n)}$ is a vector of the displacements w, u, φ for all beam segments in each beam section, **M** is the mass matrix and $\mathbf{F}^{n}$ contains all contributions from applied loads. The stiffness matrix $\mathbf{K}^{n}$ depends on time due to the non-linearity of the interfaces. The time integration technique is based on the implicit, unconditionally stable, alpha-method of Chung and Hulbert [14], which maximizes numerical dissipation of high-frequency oscillations. The regions of contact and cohesion, which are unknown *a priori*, are defined through an iterative numerical procedure.

6 RESULTS

Some general features of the response of the delaminated beam-foundation system can be observed by considering the response of the system in the fully elastic regime, when the foundation has not yet reached the yielding limit. The dashed lines in the diagram of Fig. 2 show the dimensionless energy release rate of a single delamination crack, located at the lower third of the beam thickness above the foundation, in a beam that lies on an elastic foundation with modulus K and subjected to a concentrated force per unit width P at the free end. The energy release rate is presented as a function of the normalized length of the delamination and for different values of the dimensionless group Kh/E. The group is inversely proportional to the normalized length of the oscillations of the beam on the elastic foundation, $\lambda/h = \pi^{-1}\sqrt[4]{E/3Kh}$, and is therefore named core-skin stiffness ratio in the following.

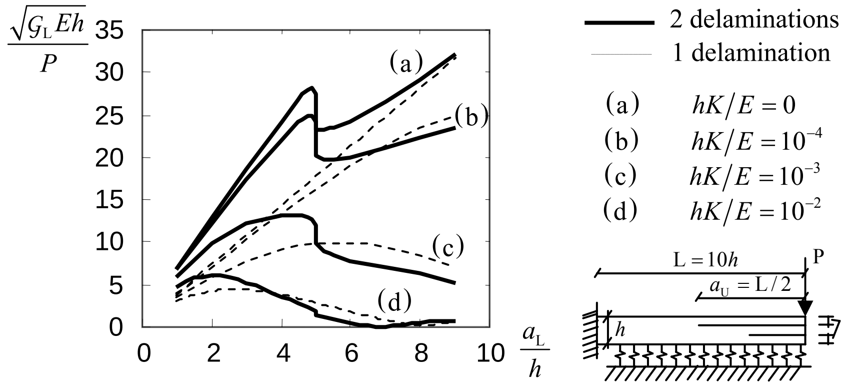

Fig. 2 Dimensionless energy release rate as a function of delamination length in a cantilever beam on an elastic foundation with one (dashed lines) and two (solid lines) delaminations.

The diagram shows that the main effect of the presence of the elastic foundation is to shield the delamination crack tip; this effect increases with the ratio hK/E. As this stiffness ratio grows above 10^{-4}, a local maximum of the energy release rate appears; further increase of the stiffness ratio moves the position of the local maximum towards the loaded end of the beam and a minimum appears close to the other end. The presence of a local minimum of the energy release rate is a general feature of the response of sufficiently long beams and represents an energy barrier to crack propagation.

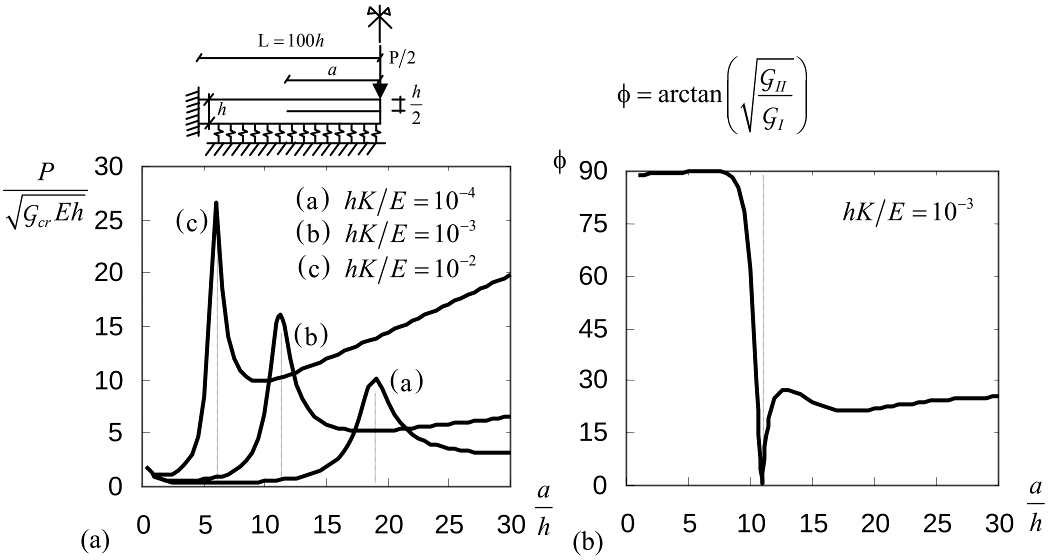

Fig. 3 (a) Dimensionless critical load for the propagation of a single midplane crack in a beam with a high length to thickness ratio on an elastic foundation (Fracture criterion: $\mathcal{G} = \mathcal{G}_I + \mathcal{G}_{II} = \mathcal{G}_{cr}$ with $\mathcal{G}_{cr}$ the fracture energy); (b) amount of mode II to mode I defined by the phase angle as a function of the delamination length.

Figure 3a shows the critical load for the propagation of a single central midplane crack in a clamped-clamped beam with a high length to thickness ratio for different stiffness ratios hK/E. Crack propagation is unstable for short crack lengths, then it becomes stable; the critical load increases up to a maximum value for a delamination length that corresponds to the position of the energy barrier. This characteristic length separates two different crack tip conditions: almost pure mode II conditions when crack lengths are shorter than the characteristic length; mixed mode conditions, with a prevalence of mode I, when crack lengths are longer (Fig. 3b).

The effects of the through-thickness position of the delamination on the critical load of the same system are shown in Figure 4. The diagram highlights that delaminations closer to the foundation propagate more easily. This behavior is observed when the crack length is close to or longer than the characteristic length. This trend is observed also in multiply delaminated systems, where the delaminations closer to the core are typically under more critical conditions. In addition, the diagram shows that the characteristic delamination length also depends weakly on the through thickness position of the delaminations.

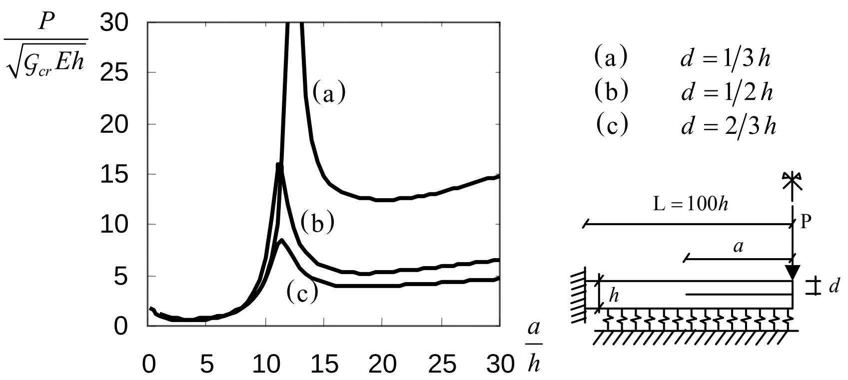

Fig. 4 Dimensionless critical load for the propagation of a single crack in a beam with high length to thickness ratio on an elastic foundation for different through thickness positions of the delamination. (Fracture criterion: $\mathcal{G} = \mathcal{G}_I + \mathcal{G}_{II} = \mathcal{G}_{cr}$ with $\mathcal{G}_{cr}$ the fracture energy)

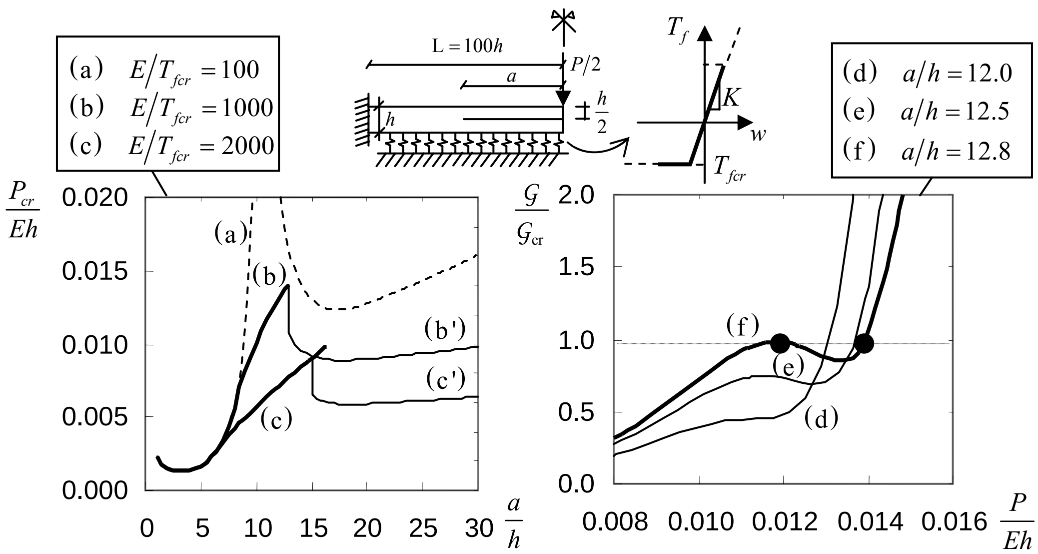

Fig. 5 (a) Dimensionless critical load for the propagation of a central, mid-plane crack in a clamped-clamped beam on an elastic-perfectly plastic foundation for different elastic limits. (Fracture criterion: $\mathcal{G} = \mathcal{G}_I + \mathcal{G}_{II} = \mathcal{G}_{cr}$ with $\mathcal{G}_{cr}$ the fracture energy); (b) normalized energy release rates as functions of the applied load for different delamination lengths and $E/T_{cr}^{f} = 2000$.

The existence of an elastic limit in the core response modifies the response of the system. This is shown in the diagram of Figure 5a where the critical load for the propagation of a central, midplane delamination crack in a clamped-clamped beam lying on an elastic-perfectly plastic foundation is shown by the solid curves for different elastic limits T_{fcr}. The main effect is an overall reduction of the critical load with respect to a fully elastic system (shown in the diagram with a dashed line). On increasing the delamination length, the critical load is given by the fully elastic load until the elastic limit is reached; afterwards, the curves deviate from the elastic solution and show a critical load that grows up to a maximum value after which the critical load decreases. The description of the evolution of the propagation for delaminations longer than this limit is still under study.

The diagram also shows the critical load for the initial propagation of a delamination; this load is described by the solid thick lines up to the delamination length where the thin lines begin and then by the thin lines. The curves show a discontinuity in the critical load. In addition, the solid lines overlap the thin lines for a certain range of delamination lengths. Within this range, the critical load for the initial propagation of a crack is different from the critical load needed to propagate the crack during its progressive growth from a different initial length. This behaviour finds an explanation in Figure 5b, where the energy release rates of delamination cracks of different lengths are shown as functions of the applied load. The diagram shows that the energy release rate is not always a monotonic function of the applied load and can have relative maxima and minima. As a consequence, a given fracture energy can correspond to different loads. The lower of these loads is the critical load for initial propagation while the higher one is reached during the propagation from an initially shorter delamination.

An example of the effects of the interaction of multiple delaminations on the energy release rate is shown in Fig. 2 (solid lines), where the normalized energy release rate of the lower delamination in the delaminated beam shown in the figure is shown as a function of its normalized length. The presence of an upper delamination of fixed length deeply modifies the energy release rates of the lower delamination compared to the single delamination solution (shown by the dashed lines): shielding and amplification effects are present and depend on the relative positions of the two delaminations. In addition, as the foundation stiffness increases with respect to the beam stiffness, the sudden transition that occurs when the delamination tips come close to each other gets smaller and then becomes negligible.

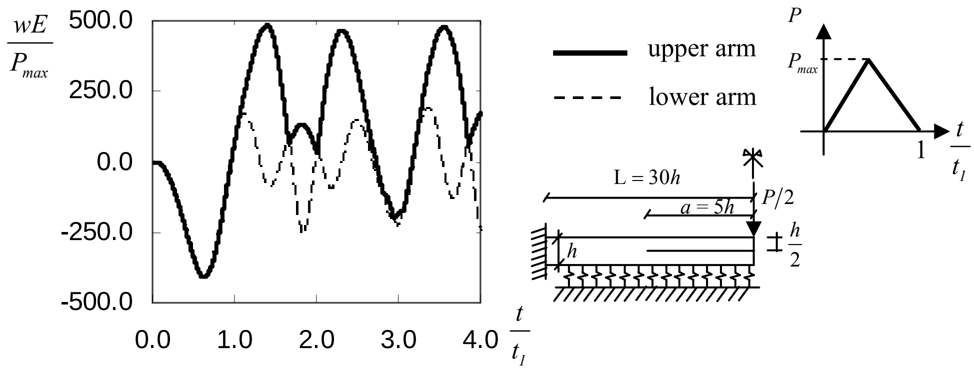

Fig. 6 Time history of the displacements of the delaminated arms at the load point in a beam with a central mid-plane delamination on an elastic foundation subject to a triangular pulse load; stationary case (t_1 is he period of the first mode of vibration of the system where delamination openings are not allowed)

The response of the sandwich system when subject to dynamic loadings shows some important differences with respect to the static case. Figure 6 depicts the time history of the load point displacements of a clamped-clamped beam with a single mid-plane delamination crack and lying on an elastic foundation. The delamination crack is stationary and the beam subjected to a triangular pulse force applied at mid-span. The diagram shows that in the free vibration phase the upper and lower arms of the delaminated beam oscillate with different frequencies and amplitudes. Specifically, the upper arm has larger and slower oscillations than the lower arm, which is constrained to the foundation; the delamination opens as a consequence. This phenomenon generates a strong mode I at the delamination crack that is not present in a static case.

The effects of this dynamic mode I regime are shown in Figure 7 whose diagrams describe the time histories of the displacements of the delaminated arms of the same beam and of the delamination length when the delamination is assumed to propagate. After a first phase of crack propagation under mode II conditions during the forced vibration phase, the remaining of crack growth is dominated by strong mode I conditions. The load point displacements show that the amplitude of the oscillation of the upper arm of the delaminated beam is one order of magnitude higher than that of the lower arm. Similar opening phenomena can be observed in the lower delamination of multiply delaminated systems. As a general remark, the opening phenomena due to the different behaviour of the lower arm that is constrained to the foundation trigger propagation phenomena that differ from those observed in the static case and that dominate the fracture process.

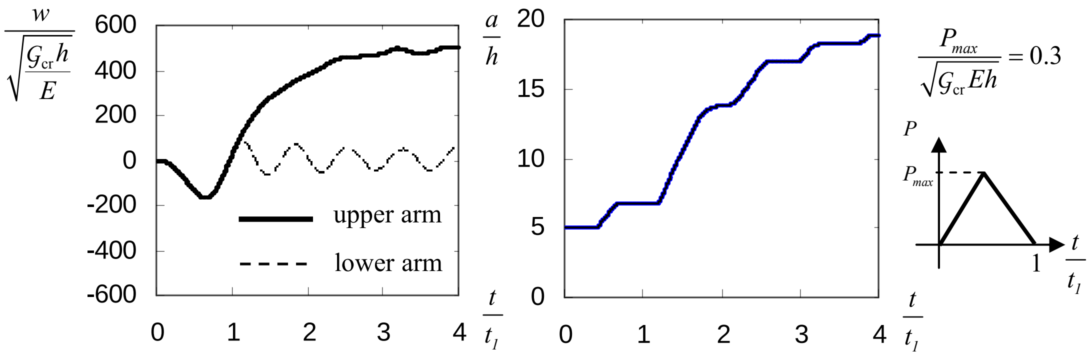

Fig. 7 (a) Time history of the displacements of the delaminated arms at the load point in a beam with a central delamination subject to a triangular pulse force applied at the mid-span (see Fig. 6 for the beam details; t_1 is period of the first mode of vibration of the system where delamination openings are not allowed); (b) time history of the crack length.

7 CONCLUSIONS

The work deals with the problem of the interaction of different damage mechanisms in face sheets and core of composite sandwich beams subject to static and dynamic out-of-plane loadings. The schematic of a delaminated beam, which represents the upper face sheet, on a nonlinear Winkler foundation, which represents the core, has been analysed.

The results from static analyses in a fully elastic regime show a generalized phenomenon of shielding of the fracture parameters that is controlled by the foundation-beam stiffness ratio and by the through-thickness position of the delaminations; delaminations close to the foundation tend to be less shielded as well as delaminations in beams with stiffer softer cores. For long enough beams, a local minimum of the energy release rate as a function of the delamination length appears at a characteristic distance from the applied load. This minimum represents a localized energy barrier to crack propagation. The barrier is described by a local sharp maximum in the curve that relates the critical load for crack propagation to crack length. After the maximum, the critical load shows an almost linear dependence on the delamination length. The introduction of an elastic limit in the response of the foundation reduces the energy barrier and the overall shielding of the crack tip.

The results from dynamic analyses show that inertia effects strongly modify the crack tip conditions and may reduce the effects of the energy barrier observed in the quasi-static cases. During the free vibration phase, after the load has been removed, the interaction with the core generates oscillations in the arms of the delaminated beam that are characterized by different frequencies and amplitudes and induce openings of the delaminations. These openings lead to important mode I crack tip conditions that typically favour crack propagation.

Acknowledgements: The authors acknowledge support by the U.S. O.N.R. through Contract no. N00014-05-1-0098, administered by Dr. Y.D.S. Rajapakse.

References

[1] Tagarielli, V.L., Deshpande V.S., Fleck N.A. 2007. "The dynamic response of composite beams to transverse impact". *Int. J. Solids Struct.* 44:2442-2457.

[2] Steeves C.A., Fleck N.A. 2004. "Collapse mechanisms of sandwich beams with composite faces and a foam core, loaded in three-point bending. Part II: experimental investigation and numerical modelling". *Int. J. Mech. Sci.* 46:585

[3] Gdoutos E.E., Daniel I.M., Wang K.A. 2003. "Compression facing wrinkling of composite sandwich structures". *Mech. Mat.* 35:511-522.

[4] McCormack T.M., Miller R., Kesler O., Gibson L.J. 2001. "Failure of sandwich beams with metallic foam cores". *Int. J. Solids Struct.* 38:4901-4920.

[5] Steeves C.A., Fleck N.A. 2004. "Collapse mechanisms of sandwich beams with composite faces and a foam core, loaded in three-point bending. Part I: analytical models and minimum weight design". *Int. J. Mech. Sci.* 46:561-583.

[6] Kim J., Swanson S.R. 2001. "Design of sandwich structures for concentrated loading". *Comp. Str.* 52:365-373.

[7] Andrews, M.G., Massabò, R. and Cox, B.N. 2006. "Elastic interaction of multiple delaminations in plates subject to cylindrical bending". *Int. J. Solids Struct.* 43(5):855-886.

[8] Andrews, M.G., Massabò R., Cavicchi, A. and Cox, B.N. 2009. "Dynamic interaction effects of multiple delaminations in plates subject to cylindrical bending". *Int. J. Solids Struct.* 46:1815-1833.

[9] Andrews, M.G. and Massabò, R. 2007. "The effects of shear and near tip deformations on energy release rate and mode mixity of edge-cracked orthotropic layers". *Eng. Fracture Mechanics*. 74:2700-2720.

[10] Alfano, G and Crisfield, MA. 2001. "Finite element interface models for the delamination analysis of laminated composites: Mechanical and computational issues". *Int. J. for Numerical Methods in Engineering*. 50(7):1701-1736.

[11] Zou, Z., Reid, S.R., Soden, P.D. and Li. S. 2001. "Mode separation of energy release rate for delamination in composite laminates using sublaminates". *Int. J. Solids Struct*. 38:2597-2613.

[12] Ortiz, M. and Suresh, S. 1993. "Statistical Properties of Residual-Stresses and Intergranular Fracture in Ceramic Materials". *J. Appl. Mech*. 60(1):77-84.

[13] Bruno, D., Greco, F. and Lonetti, P. 2003. "A coupled interface-multilayer approach for mixed mode delamination and contact analysis in laminated composites". *Int. J. Solids Struct.* 40:7245-7268.

[14] Chung, J. and Hulbert, G.M.. 1993. "A time integration algorithm for structural dynamics with improved numerical dissipation - the generalized-alpha method". *J. Appl. Mech.* 60 (2):371-75.